Available online at www.sciencedirect.com
ScienceDirect
Journal of Hazardous Materials 150 (2008) 37–45
Journal of Hazardous Materials
www.elsevier.com/locate/jhazmat

Oxidative decolorization of methylene blue using pelagite

Mao-Xu Zhu [a,*], Zheng Wang [a], Liang-Yong Zhou [b]

[a] Key Laboratory of Marine Chemistry Theory and Technology, Ministry of Education, Ocean University of China, Qingdao 266100, PR China
[b] Qingdao Institute of Marine Geology, China Geological Survey, Qingdao 266071, PR China

Received 3 November 2006; received in revised form 8 April 2007; accepted 17 April 2007
Available online 20 April 2007

Abstract

Pelagite generally has large surface area and high adsorbing and oxidizing reactivity due to highly amorphous nature, and high reducing potential of Mn (hydro)oxide phases present in it. In the present study, pelagite, collected from the East Pacific Ocean, was tested as a potential oxidant for decolorization of methylene blue (MB) in a batch system under air-bubbling and motor-stirring conditions. The effects of suspension pH (3.0–10.0), MB concentration (10–100 mg L^{-1}) and loading (0.2–3.0 g L^{-1}), and particle size (100–200 mesh) of pelagite on kinetics of MB decolorization were assessed. Results show that in typical concentration range of dye wastewaters (10–50 mg L^{-1}), pelagite can be used as a highly efficient material for oxidative degradation of MB. MB decolorization was through a surface mechanism, that is, formation of surface precursor complex between MB and surface bound Mn(III, IV) center, followed by electron transfer within the surface complex. Iron (hydro)oxide phases present in the pelagite did not play an important role in MB decolorization. Suspension pH exerted double-edged effects on MB decolorization by influencing the formation of surface precursor complex, and reducing potential of the system. Kinetic rate of MB decolorization is directly proportional to saturation degree of available reaction sites by MB adsorption. At the initial and later stages, the kinetics for MB decolorization with respect to MB concentration, pelagite loading, and particle size could be described separately using two pseudofirst rate equations, except at very high pelagite loading (3.0 mg L^{-1}). Accumulation of Mn^{2+} and probably some organic intermediates exerted marked inhibitory effect on MB decolorization. Vigorous dynamic condition was favorable for MB decolorization. The presence of oxygen could enhance MB decolorization to a limited extent.

Keywords: Pelagite; Methylene blue; Oxidative decolorization; Adsorption; Surface complex; Degradation

1. Introduction

Due to large surface area and high scavenging capabilities, the presence of only tiny amounts (e.g. a fraction of a weight percent of soil or sediment) of manganese (Mn) oxide minerals might be adequate to control distribution and migration of heavy metals, and other trace elements [1]. Manganese oxides are also powerful oxidants due to high reducing potential. It is recognized that Mn oxides can oxidize many inorganic compounds including Co(II) [2], Cr(III) [3], As(III) [4], Sb(III) [5], and Se(IV) [6], and a wide spectrum of natural and xenobiotic organic compounds such as catechol, quinines, substituted phenols, aromatic amines, pesticides, and explosives (e.g. TNT) [7–11]. It has been reported that abiotic degradation of a number of organic pollutants by Mn oxides is an important pathway for natural attenuation of those pollutants in soils and sediments [12].

For pollution remediation purposes, land-born natural Mn ores, synthetic nascent state Mn oxides, and materials coated/modified with Mn oxides have been tested as scavenger for removal of Pb^{2+}, Cd^{2+}, Cu^{2+}, 17α-ethynylestradiol [13–16], as oxidant for degradation of organic pollutants [17,18], and as oxidant and/or adsorbent for removal of As(III) and As(V) [19].

Pelagite, also referred to as marine Mn nodule, is an autogenic complex material, widely distributed, and vastly accumulated in the sea floor 4000–6000 m deep in the Pacific Ocean, Indian Ocean, and Atlantic Ocean [20]. It is consisted primarily of Mn and Fe (hydro)oxides [21]. Pelagite and its residues after extraction of valuable metals were found to be good adsorbents for a number of pollutants such as Zn^{2+}, Pb^{2+}, Ni^{2+}, phosphate and selenite, and thus, could be used in wastewater treatment [22–26]. The crystallinity of pelagite is much

* Corresponding author. Tel.: +86 532 66782513; fax: +86 532 66782540.
E-mail address: zhumaoxu@ouc.edu.cn (M.-X. Zhu).

0304-3894/$ – see front matter © 2007 Elsevier B.V. All rights reserved.
doi:10.1016/j.jhazmat.2007.04.042

lower than that of land-born Mn ores. Therefore, pelagite has a larger surface area, stronger adsorbing power, and higher redox activity. These characteristics plus generally high reducing potential of Mn (hydro)oxides (main compositions present in pelagite) interest the authors to evaluate possible application of pelagite as an effective oxidant for degradation of organic contaminants in water treatment because it is accepted that, for a heterogeneous redox reaction, high adsorbing power, and redox activity of the solid phases involved are two critical factors influencing kinetic rate of the reaction. In this study, decolorization of methylene blue (MB), a cationic dye, as a model organic matter was investigated using pelagite as an oxidant.

2. Materials and methods

2.1. Materials

Pelagite collected from the East Pacific Ocean were sonically cleaned in deionized water followed by drying at 60 °C for 48 h, and then mechanically ground to pass through 100, 100–120, 140–160, and 200 mesh sieve for use. Particle size and average surface area of the pelagite are given in Table 1. Micromorphology of the pelagite (100 mesh) and element contents were previously determined using scanning electron microscopic observation and energy dispersive X-ray microanalysis, respectively [27]. The pelagite was also subjected to X-ray diffraction (XRD) analysis on a Rigaku D/max-rB diffractometer (Rigaku Corp., Japan) (Cu Ka, 40 kV, 100 mA, 7 °C min^{-1}) to ascertain the mineral phases present in it.

MB (purity >98%) was purchased from the Tianjin Guangcheng chemical reagent Co. Ltd., and used without further purification. The chemical structure of MB is shown in Fig. 1. Stock solution (400 mg L^{-1}) of the dye was prepared by dissolving MB in deionized water. Dye solutions of desired pH values were obtained by adjustment using dilute HCl or NaOH solutions.

2.2. Experimental procedure and analytical methods

Individual decolorization experiment was conducted using a batch method in a constant temperature water bath at (25 ± 0.5) °C and under motor-stirring (550 rpm) and air-bubbling (flow rate 32 mL s^{-1}) conditions. While stirring and air-bubbling, 0.3 g (i.e. 0.6 g L^{-1}) pelagite, unless otherwise stated, was added into a flask reactor containing 500 mL MB solution (concentrations and pH ranging from 10 to 100 mg L^{-1} and from 3.0 to 10.0, respectively). System pH as the reactions proceeded was not controlled, since inorganic ionic compounds added for pH adjustment or buffering may adsorb on surface of the pelagite and organic buffer agents used may be oxidized, which would substantially affect MB degradation [11]. At specific time intervals (10 min–1 h) aliquots of 10-mL suspension were sampled using a syringe and filtrated through a 0.22-μm syringe-end filter. Filtrate pH was determined immediately after filtration. The filtrates were then stored at 4 °C until determination of MB concentration using a Hewlett-Packard 8453 UV–VIS spectrophotometer at λ_{max} = 665 nm. To evaluate the extent of MB mineralization, total organic carbon (TOC) contents in filtrates of some selected runs were determined using a TOC-V_{CPN} total carbon analyzer (Shimadzu Corp. Japan). Also, Mn and Fe concentrations in filtrates of some selected runs were determined using a flame AAS (Thermo Electron Co. USA) in order to glean information about the mechanism of MB decolorization. The filtrates for Mn and Fe determination were acidified using three droplets of 1:1 HNO_3 to around pH 1.0 immediately after filtration. The influence of pH (3.0–10.0), dye concentration (10–100 mg L^{-1}), loading (0.2–3.0 g L^{-1}) and particle size (100–200 mesh) of the pelagite, on oxidative decolorization of MB were assessed. To evaluate the effects of dynamic conditions, and the presence of oxygen molecule on MB decolorization, 500 mL MB solution (10 mg L^{-1}) were reacted with 0.3 g pelagite in a flask reactor under different dynamic conditions: shaking (rotary shaker, 145 rpm) *versus* motor-stirring (550 rpm), air-bubbling (32 mL s^{-1}) *versus* nitrogen bubbling (32 mL s^{-1}) conditions, for comparison purpose.

To assess the feasibility for consecutive reuse of pelagite and the effects of reaction products on MB decolorization, MB was treated with the pelagite in a consecutive batch system. Initially, 1.5 g pelagite was added into a flask reactor containing 500 mL MB (50 mg L^{-1}, pH 3.0) under motor-stirring (550 rpm) and air-bubbling (32 mL s^{-1}) conditions. Experimental procedure and sampling method were similar to those described above. When a high decolorization percentage (≥95%) was obtained, required volume of fresh MB solution (400 mg L^{-1}) was added to reach a concentration similar to that in the initial system, followed by rapid pH adjustment to about 3.0 using HNO_3 solution. In predetermining the volume of fresh MB solution required to add, residual MB concentration in the reaction system was ignored. When a high decolorization percentage (≥95%) was obtained again after the second round addition, a third round addition of fresh MB solution and pH adjustment was followed.

All the experiments were run in duplicate and all the data presented were the averages of duplicate analysis.

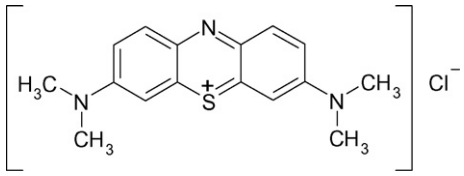

Fig. 1. Chemical structure of MB.

Table 1
Particle size and average surface area of the pelagite

Sieve mesh	Particle diameter (mm)	Average surface area (m^2 g^{-1})
100	<0.150	105
100–120	0.150–0.125	79
140–160	0.106–0.097	94
200	<0.076	115

Table 2
Element contents in the pelagite

Element	Weight (%)	Atomic (%)
C	10.16	19.94
O	32.87	48.45
Al	3.61	3.15
Si	9.93	8.34
Ca	9.71	5.71
Mn	28.53	12.24
Fe	4.62	1.95
Cu	0.58	0.21
Total	100.00	

3. Results and discussion

3.1. Characterization of pelagite

Element contents in the pelagite are shown in Table 2. The result suggests that, among the metal elements, the content of Mn is far higher than that of the others. From the pattern of XRD analysis (Fig. 2), the peaks at *d*-spacing 9.77 and 4.83 Å can be assigned to todorokite; the peaks at *d*-spacing 7.25 and 3.59 Å can be assigned to birnessite. The peaks at *d*-spacing 2.44 and 1.42 Å can be assigned either to vernadite, todorokite or birnessite [28], but a further identification is difficult due to weak and broad peaks. Todorokite is well crystalline based on its strong and sharp peak at *d*-spacing 9.77 Å. Other Mn oxides are poorly crystalline. Quartz at *d*-spacing 3.35 Å exhibits the sharpest peak due to its perfectly crystalline nature. Iron (hydro)oxides usually coexist with Mn (hydro)oxides in pelagite and the content of Fe (4.62 wt.%) is not very low in the pelagite studied as shown in Table 2, but no peak of Fe (hydro)oxide mineral phases was observed due probably to highly amorphous nature of the phases.

3.2. Effect of initial MB concentration

The effect of MB concentration on decolorization of MB at initial pH 3.0 is shown in Fig. 3. The efficiency of MB decolorization decreased markedly with increasing concentration of MB. For example, the percentage of MB decolorization reached

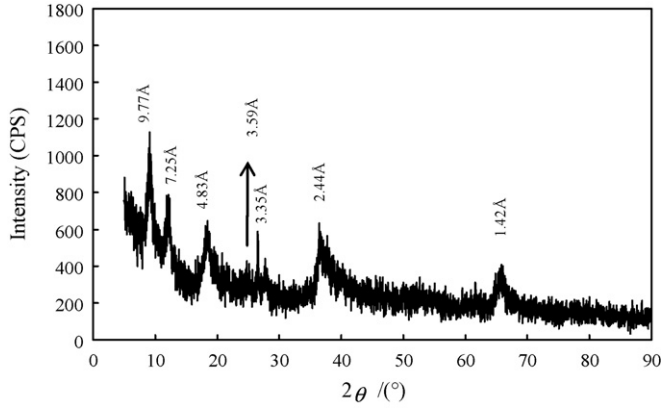

Fig. 2. XRD pattern of pelagite.

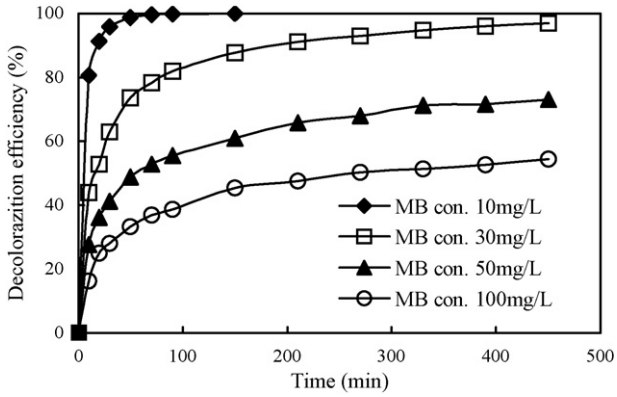

Fig. 3. Effect of initial concentration of MB on decolorization at initial pH 3.0 and pelagite loading 0.6 g L^{-1}.

90% over 20 min and color almost completely disappeared over 1 h when initial MB concentration was 10 mg L^{-1}. When initial MB concentration was 100 mg L^{-1}, however, the percentage was only 50% over 7.5 h.

It has been well established that oxidative degradation of organic matter by Mn oxides is via a surface mechanism [29], that is, the organic compound is adsorbed on surface of Mn oxides to form a surface precursor complex, electron transfer then occurs within the surface complex from organic reductant to the surface-bound Mn(III, IV), followed by release of organic oxidation products and Mn(II) arising from reductive dissolution of Mn oxides. The formation of surface precursor complex and/or electron transfer may be rate-limiting steps, depending on reaction conditions. As will be experimentally confirmed later, MB decolorization by the pelagite is most likely to follow this surface mechanism, as do many other organic pollutants [8–10]. It follows that surface reactivity and the number of available adsorption sites are two critical factors controlling oxidative decolorization of MB. As can be seen in Fig. 3, at a fixed loading of the pelagite (0.6 g L^{-1}), MB decolorization decreased with an increase in initial MB concentrations, suggesting that reactive adsorption sites were saturated with MB at low MB concentration, additional MB would not further increase the formation of precursor complex, and thus, the decolorization percentage decreased with an increase in MB concentration.

3.3. Effect of loading and particle size of pelagite

The effect of pelagite loading on MB decolorization and increase in TOC removal with reaction time in selected runs are illustrated in Fig. 4(a and b). Also shown in Fig 4b, is corresponding color removal for comparison purpose. When 3.0 g L^{-1} of the pelagite was used, the percentage of MB decolorization increased rapidly over the initial time period, approaching 90% over 30 min, and the color was almost completely eliminated over 100 min, whereas the efficiency decreased substantially when 0.2 g L^{-1} of the pelagite was employed.

The effect of particle size of the pelagite on MB decolorization and corresponding variation in soluble Mn with time are

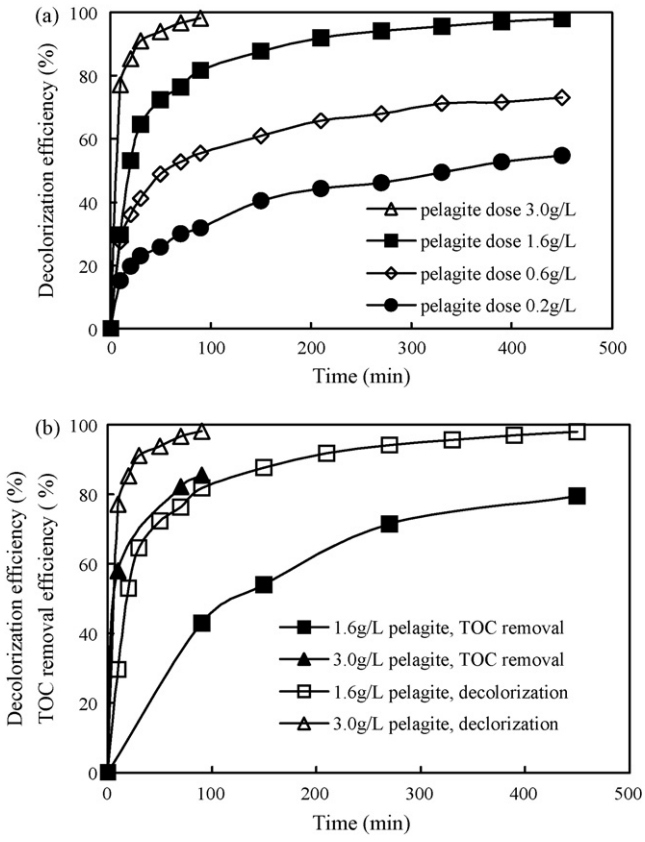

Fig. 4. Effect of pelagite loading on decolorization of MB (a), and comparison of TOC removal with decolorization efficiency (b) at initial concentration of MB 50 mg L^{-1} and initial pH 3.0.

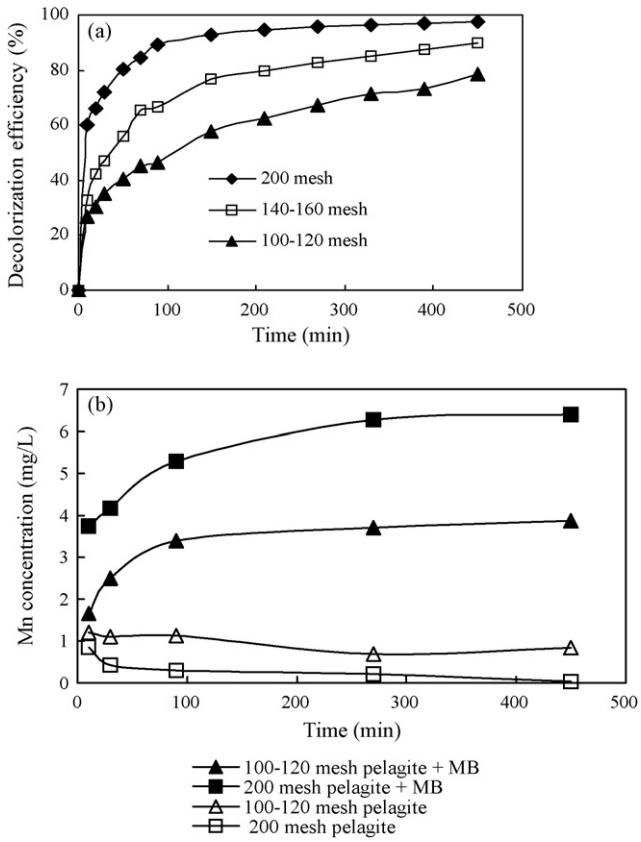

Fig. 5. Effect of pelagite particle size on decolorization of MB (a), and on Mn dissolution at initial pH 3 (b) at initial concentration of MB 30 mg L^{-1}, initial pH 3.0 and pelagite loading 0.6 g L^{-1}.

shown in Fig. 5(a and b). It can be seen that a decrease in particle size of the pelagite significantly enhanced the efficiency of MB decolorization. Based on the surface oxidation mechanism described in Section 3.2, the more the loading of the pelagite was used, the more the active surface sites for the formation of surface precursor complex were available, and therefore the higher the percentage of MB decolorization would be achieved. Similarly, with a decrease in particle size, specific surface area of the pelagite, and thus, the total number of active surface sites increased, which could also greatly enhance the efficiency of MB decolorization as shown in Fig. 5a.

TOC removal increased with the increase in decolorization, but markedly lower than the latter (Fig. 4b). For example, when the decolorization percentage was 98% over 100 min, the percentage of TOC removal was less than 80%. But the difference diminished as the reaction prolonged, which seemingly suggested that chromophoric moieties in MB molecules were preferentially broken down, followed by slow mineralization of some organic intermediates as the reaction progressed. On basis of TOC removal, the efficiency of MB mineralization in the present study is generally high, comparable to some advanced oxidation process. For example, for photoelectrochemical degradation of 1.0 mmol L^{-1} MB (200 mL), the percentage of TOC removal was 81% over 30 min [30], the percentage for photocatalytic degradation of 100 mg L^{-1} MB (50 mL) in TiO_2 suspension was 45% over 15 min [31].

Oxidative decolorization mechanism of MB on the surface of the pelagite was further confirmed by the result shown in Fig. 5b. In the presence of H^+ (pH 3.0) alone, soluble Mn concentration was very low and remained almost unchanged with time, suggesting that the solubility of Mn oxides present in the pelagite was very limited under the inorganic acid condition of this study. In contrast, in the presence of MB, soluble Mn concentration was obviously enhanced, and progressively increased with time, particularly for pelagite of fine particle size. This could be attributed to Mn^{2+} release arising from reductive dissolution of Mn (hydro)oxides with MB as electron-donator, based on much discussion in literature [12,29]. It should be noted that soluble Mn(II) in the solutions was a net result of reductive dissolution and surface adsorption because Mn^{2+} is readily adsorbed on Mn and Fe (hydro)oxides [12]. In the present study, Fe (hydro)oxides present in the pelagite were believed not to play an important role in oxidative decolorization of MB because no measurable soluble Fe in the solution was detected, suggesting no or very limited (considering adsorption of released Fe^{2+}) reductive dissolution of Fe (hydro)oxides. This is not surprising because reducing potentials of Fe (hydro)oxide minerals are far lower than those of Mn(III, IV) (hydro)oxide minerals (Table 3). Thermodynamically, electron transfer occurs preferentially from electron-donator (MB) to electron-acceptor with the highest reducing potential among coexisting oxidizing agents.

Table 3
Standard reducing potential for some Fe(III) and Mn(III, IV) (hydro)oxide minerals

Redox couple	Redox reaction	Reducing potential φ° (V)
γ-MnOOH/Mn^{2+}	γ-MnOOH (s) + $3H^+ + e^- \rightarrow Mn^{2+}$ (aq) + $2H_2O$	1.50 [32]
γ-MnO_2/Mn^{2+}	γ-MnO_2 (s) + $4H^+ + 2e^- \rightarrow Mn^{2+}$ (aq) + $2H_2O$	1.27 [32]
δ-MnO_2/Mn^{2+}	δ-MnO_2 (s) + $4H^+ + 2e^- \rightarrow Mn^{2+}$ (aq) + $2H_2O$	1.29 [32]
α-FeOOH/Fe^{2+}	α-FeOOH (s) + $3H^+ + e^- \rightarrow Fe^{2+}$ (aq) + $2H_2O$	0.656 [33]
γ-FeOOH/Fe^{2+}	γ-FeOOH (s) + $3H^+ + e^- \rightarrow Fe^{2+}$ (aq) + $2H_2O$	0.757 [33]
α-Fe_2O_3/Fe^{2+}	α-Fe_2O_3 (s) + $6H^+ + 2e^- \rightarrow 2Fe^{2+}$ (aq) + $3H_2O$	0.655 [33]

3.4. Effect of initial pH

The effect of initial pH on MB decolorization at initial MB concentration 30 mg L^{-1} and pelagite loading 0.6 g L^{-1} is illustrated in Fig. 6. At pH less than 4, the efficiency of MB decolorization increased with a decrease in initial pH. At pH 4 to 10, however, pH exerted only limited effect on the decolorization.

The formation of surface precursor complex, one of kinetic rate-limiting steps in heterogeneous oxidative degradation of organic pollutants, is closely related to the nature of surface charge. The amount of surface charge on the pelagite is determined by protonation or deprotonation process, depending on suspension pH. In the present study, pH at zero point of charge (pH_{zpc}) of the pelagite was determined to be 4.7 using a simplified method [34], which is similar to that (pH_{zpc} 4.5) of pelagite collected from the Indian Ocean, as determined using the traditional potentiometric acid–base titration method [22,23]. Theoretically, at pH lower than the pH_{zpc} 4.7, the surface of the pelagite is positively charged due to protonation, and the positive charge increases with deceasing suspension pH, which does not favor MB adsorption and formation of surface precursor complex due to electrostatic repulsion; at pH higher than 4.7, the surface is negatively charged due to deprotonation and negative surface charge increases with increasing suspension pH, which is conducive to the formation of surface precursor complex. Although low pH impeded the formation of surface precursor complexes, high H^+ concentration, however, could improve reducing potential of the system according to the Nernst Equation. An increase in suspension pH would decrease oxidizing power of the system. On the other hand, the increase in formation of surface precursor complex due to pH increase could compensate for the reduction in oxidizing power of the system to some extent. One may conclude that suspension pH exerted two double-edged effects on MB decolorization. The result of the present study indicated that, even though a decrease in initial pH suppressed MB adsorption on the pelagite, an increase in reducing potential of the system still entailed an increase in MB decolorization over the range of pH less than 4, which strongly suggested that it was heterogeneous surface oxidation but not pure adsorption that was the principal mechanism for MB decolorization. To date, it is not likely to accurately determine the saturation concentration of MB on pelagite surface and the relative contribution of pure surface adsorption and oxidative degradation to MB decolorization because surface redox takes place immediately after adsorption of organic matter [7]. Limited influence of initial pH on MB decolorization at pH greater than 4 implied that the two opposite effects pH exerted were likely to approximately counteract with each other.

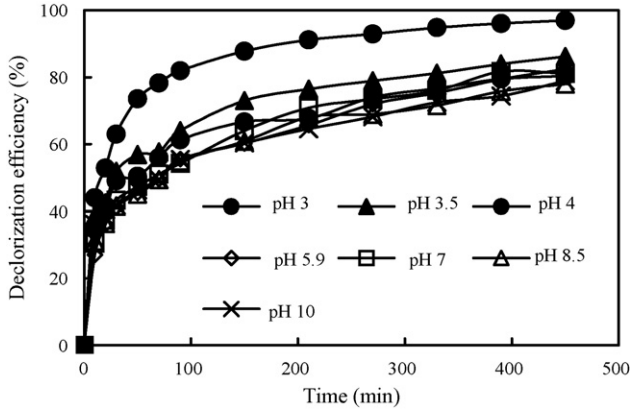

Fig. 6. Effect of initial pH on decolorization of MB at initial concentration of MB 30 mg L^{-1} and pelagite loading 0.6 g L^{-1}.

3.5. Kinetics of MB decolorization

Factors influencing MB oxidative degradation could be quantitatively assessed using kinetic rate. Suitable rate expressions obtained from kinetic modeling can also allow insight into possible reaction mechanisms. Several authors reported that, in pH-buffered system, the kinetics of oxidative degradation of a number of organic pollutants by Mn oxides was first-order with respect to organic pollutant concentration over the initial stage, but deviated from the pseudofirst-order equation as the reaction prolonged [10,35]. Without pH control as reaction proceeded, Kang et al. [11] also found oxidative degradation of 2,4,6-trinitrotoluene (TNT) by birnessite (δ-MnO_2) well followed the pseudofirst-order kinetics with respect to birnessite loading over the initial stage. Among many studies above, suspension pH was found to exert a marked influence on the overall kinetic rate for oxidative degradation of a series of organic pollutants. Probably, it is because in those studies the organic pollutants investigated were anions (or anions after ionization at pH ranges studied) that both reducing potential and formation of surface precursor complex decreased with an increase in solution pH. In those studies, no effort was made to characterize the kinetics after the initial stage of reaction probably because several complicated factors influencing the kinetic rate were involved as the reaction prolonged.

With respect to MB concentration, pelagite loading, and particle size, the kinetic data (Figs. 3, 4a and 5a) at the initial and later

stages could be fitted separately using two pseudofirst rate equations (Fig. 7), except at very high pelagite loading (3.0 mg L^{-1}), where only one pseudofirst rate equation was needed. Because surface adsorption was the first step to oxidative decolorization, MB concentration at $t = 0$ did in fact not exactly correspond to the initial bulk concentration of surface oxidation reaction, thus the data at $t = 0$ were excluded in the fitting. The higher rate constants over the initial stage (stage I) than that over the later stage (stage II) implied that different rate-limiting steps were involved in the two stages. We did not try to clarify the specific factors responsible for the decrease in rate constants over the later stage. But the decrease could be attributed partly to an increase in pH and inhibitory effect of Mn^{2+}. Suspension pH was found to increase under all experimental conditions due to H^+ consumption in the redox process. Progressive increase in pH with time would exert two double-edged effects on the decolorization. Accumulation of Mn^{2+} would compete with MB for active surface sites and block adsorption of MB, and also suppress oxidizing power of the system in terms of the Nernst equation.

Even though the increase in inhibitory effect of Mn^{2+} as well as the decrease in oxidizing power of the system due to Mn^{2+} accumulation and H^+ consumption suppressed the kinetic rate of MB decolorization over the later stage, rate constants for a given system remained constant (Fig. 7). Probably, the double-edged effects pH exerted on MB decolorization as discussed above and the formation of $Mn^{III}OOH$ resulting from surface autocatalytic oxidation of adsorbed Mn^{2+} by oxygen in the present air-bubbling system might help remain a stable rate constant. Oxygen may heterogeneously oxidize (surface autocatalytic oxidation) Mn^{2+} adsorbed on the pelagite, leading to formation of MnOOH [36]. The newly formed Mn(III) hydroxide is also an active adsorbent and oxidant, and may help improve MB adsorption and following oxidation to some extent. It has been reported that when oxygen is present and pH is above 5 oxygenation of Mn^{2+} can occur, and when pH is above 8, rate of Mn^{2+} oxidation and regeneration of Mn(III, IV) (hydro)oxides become significant [36,37].

With very high pelagite loading (3.0 g L^{-1}), the percentage of MB decolorization approached 100% rapidly (Fig. 4a). In this case, very large amount of surface sites was available to form surface complex, and probably the surface was even not saturated with MB. It is likely that a complete decolorization of MB has been rapidly achieved before an increase in pH and inhibitory effect of accumulated Mn^{2+} could exert marked influence on the overall kinetics, and therefore the kinetic data could be fitted using a single pseudofirst rate equation as shown in Fig. 7b.

As shown in Table 4, an increase in kinetic rate with increasing loadings and decreasing particle size of the pelagite was a direct and quantitative indicative of surface-dependent reaction mechanism. Also concentration-dependent kinetic rate was an indirect indicative of the same mechanism.

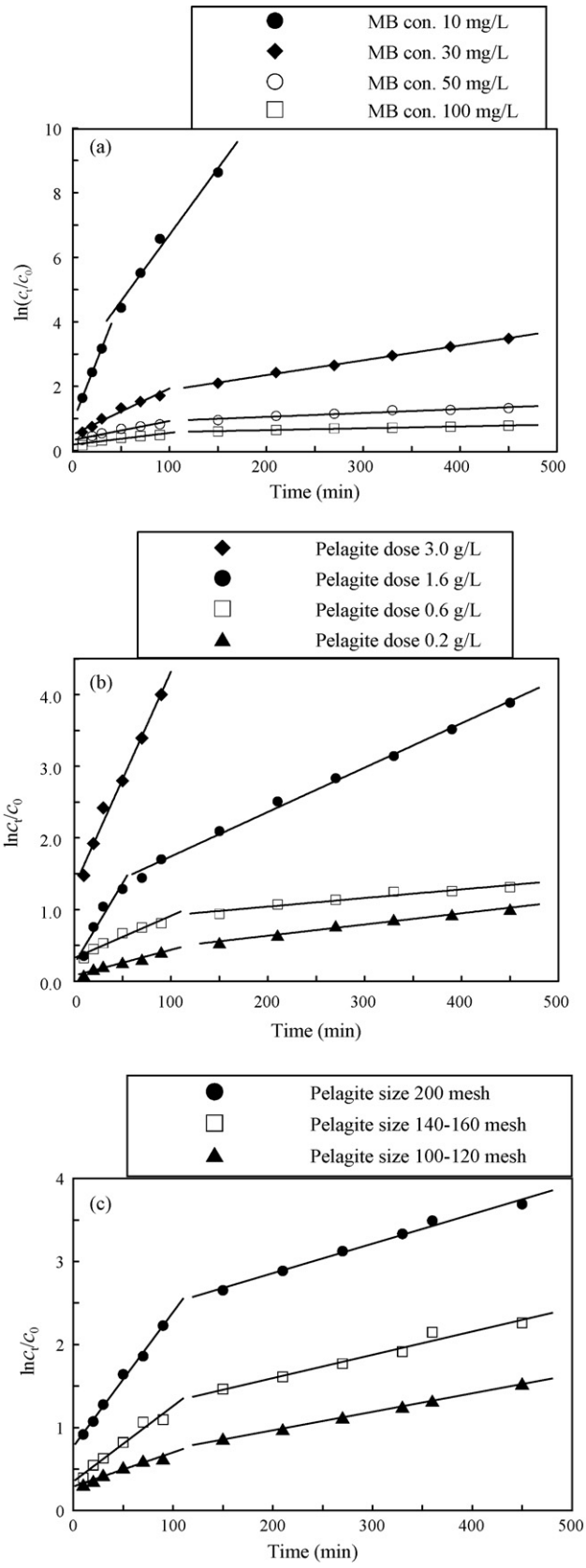

Fig. 7. Pseudofirst-order fitting of MB decolorization with respect to MB concentration (a), pelagite loading (b), and particle size (c).

3.6. Effect of dynamic conditions

The effect of dynamic conditions (shaking *versus* motor-stirring, air-bubbling *versus* nitrogen bubbling) of the reaction

Table 4
Pseudofirst-order rate constants for MB decolorization with respect to MB concentration, pelagite loading, and particle size

MB concentration	10 mg L^{-1}		30 mg L^{-1}		50 mg L^{-1}		100 mg L^{-1}	
	Stage I	Stage II	Stage I	Stage II	Stage I	Stage II	Stage I	Stage II
k (min^{-1})	7.7×10^{-2}	4.1×10^{-2}	1.4×10^{-2}	4.6×10^{-3}	5.9×10^{-3}	1.2×10^{-3}	3.6×10^{-3}	5.9×10^{-4}
SD (mg L^{-1})	9.0×10^{-5}	7.5×10^{-4}	0.03	4.2×10^{-3}	1.5	0.96	7.9	0.98
r^2	0.999	0.985	0.971	0.998	0.947	0.941	0.916	0.984

Pelagite loading	0.2 g L^{-1}		0.6 g L^{-1}		1.6 g L^{-1}		3.0 g L^{-1}
	Stage I	Stage II	Stage I	Stage II	Stage I	Stage II	
k (min^{-1})	3.6×10^{-3}	1.6×10^{-3}	5.9×10^{-3}	1.2×10^{-3}	2.3×10^{-2}	6.2×10^{-3}	3.0×10^{-2}
SD (mg L^{-1})	3.1	0.35	1.5	0.96	1.9	0.02	0.18
r^2	0.963	0.987	0.947	0.941	0.919	0.995	0.986

Particle size	100–120 *mesh*		140–160 *mesh*		200 mesh	
	Stage I	Stage II	Stage I	Stage II	Stage I	Stage II
k (min^{-1})	4.1×10^{-3}	2.2×10^{-3}	9.0×10^{-3}	2.8×10^{-3}	1.6×10^{-2}	3.6×10^{-3}
S.D. (mg L^{-1})	1.2	0.02	1.3	0.30	0.14	0.01
r^2	0.961	0.999	0.965	0.969	0.989	0.995

S.D.: standard deviation; r^2: regression coefficient.

system on MB decolorization is illustrated in Fig. 8. It can be seen that the kinetic rate for MB decolorization was higher under motor-stirring and air-bubbling (a vigorous dynamic condition) than under shaking and air-bubbling (a weak dynamic condition), particularly at the initial reaction period. This suggests that vigorous dynamic condition is favorable for the degradation reaction due probably to an enhancement in mass transfer of reactants to the surface of the pelagite and reaction products leaving from the surface to the bulk solution. Gas bubbling also enhanced the kinetic rate of MB decolorization compared with in the absence of gas bubbling, particularly at the later period of the reaction, which is speculated to be primarily the result of elevated dynamic condition, oxygen molecule itself played only a limited role because the differences in percentage of MB decolorization under air-bubbling and nitrogen-bubbling conditions were marginal. The role oxygen played might be via the mechanism of autocatalytic oxygenation of Mn^{2+} as discussed above.

3.7. Consecutive batch system for reuse of pelagite

The efficiency of MB decolorization in a consecutive batch system is shown in Fig. 9. In the first round, 95% of decolorization was obtained over 30 min for 50 mg L^{-1} of MB at initial pH 3.0 and pelagite loading 3.0 g L^{-1}. After the second round addition of fresh MB to obtain similar MB concentration and pH as in the first round, 240 min was needed to achieve 95% of decolorization, much longer than in the first round. After the third round addition of fresh MB, less than 90% of decolorization was achieved even over 350 min. It is clear that, in the consecutive system, the accumulation of Mn^{2+} and probably some organic intermediates exerted marked inhibitory effect on MB decolorization. Therefore, separation of reaction products from

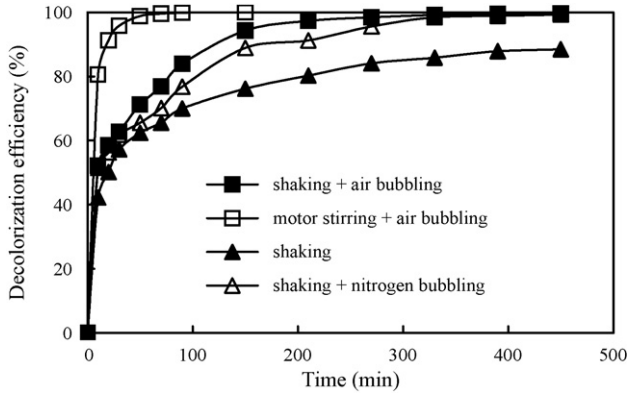

Fig. 8. Effect of dynamic condition on decolorization of MB at initial pH 3.0, initial MB concentration 10 mg L^{-1}, and pelagite loading 0.6 g L^{-1}.

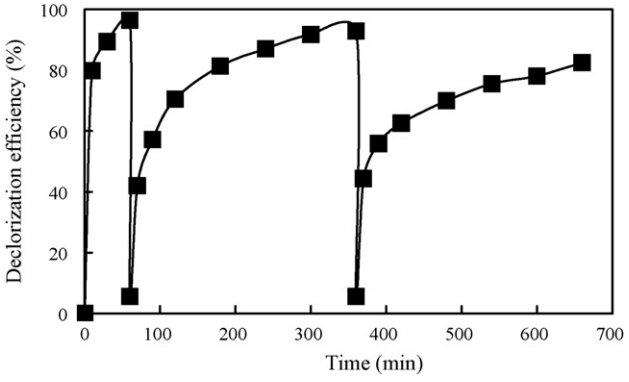

Fig. 9. Effect of consecutive batch reaction on decolorization of MB.

the system is needed to improve efficiency of MB decolorization in a consecutive system.

4. Conclusion

In typical concentration range of dye wastewaters (10–50 mg L^{-1}), pelagite is a promising material for efficient oxidative decolorization of MB, and a high extent of mineralization could be achieved. MB decolorization was through a heterogeneous oxidization mechanism. Iron oxides present in the pelagite did not play an important role in oxidative decolorization of MB. Both MB decolorization and TOC removal were enhanced significantly with an increase in loading and a decrease in particle size of the pelagite. An increase in MB concentration substantially reduced MB decolorization when adsorption sits on pelagite were saturated with MB. Suspension pH exerted double-edged effects on MB decolorization by influencing the formation of surface precursor complex and reducing potential of the system. At pH less than 4, MB decolorization increased with a decrease in initial pH, while pH exerted only limited effect on MB decolorization at pH 4–10. At the initial and later stages, the kinetic data for MB decolorization with respect to MB concentration, pelagite loading, and particle size could be described separately using two pseudofirst rate equations, except at very high pelagite loading (3.0 mg L^{-1}), where only one pseudofirst rate equation was needed. Accumulation of Mn^{2+} and probably some organic intermediates in a consecutive batch system exerted marked inhibitory effect on MB decolorization. Vigorous dynamic condition was favorable for MB decolorization. The presence of oxygen could enhance MB decolorization but to a limited extent via probably the mechanism of autocatalytic oxygenation of Mn^{2+}.

References

[1] D. Dong, L.A. Derrym, L.W. Lion, Pb scavenging from a freshwater lake by Mn oxides in heterogeneous surface coating materials, Water Res. 37 (2003) 1662–1666.
[2] A. Manceau, V.A. Drits, E. Silvester, C. Bartoli, B. Lanson, Structural mechanism of Co^{2+} oxidation by the phyllomanganate buserite, Am. Mineral. 82 (1997) 1150–1175.
[3] J.G. Kim, J.B. Dixon, C.C. Chusuei, Y. Deng, Oxidation of chromium(III) to (VI) by manganese oxides, Soil Sci. Soc. Am. J. 66 (2002) 306–315.
[4] V.Q. Chiu, J.G. Hering, Arsenic adsorption and oxidation at manganite surfaces. 1. Method for simultaneous determination of adsorbed and dissolved arsenic species, Environ. Sci. Technol. 34 (2000) 2029–2034.
[5] N. Belzile, Y.-W. Chen, Z. Wang, Oxidation of antimony(III) by amorphous iron and manganese oxyhydroxides, Chem. Geol. 174 (2001) 379–387.
[6] M.J. Scott, J.J. Morgan, Reactions at oxide surfaces. 2. Oxidation of Se(IV) by synthetic birnessite, Environ. Sci. Technol. 30 (1996) 1990–1996.
[7] C.J. Matocha, D.L. Sparks, J.E. Amonette, R.K. Kukkadapu, Kinetics and mechanism of birnessite reduction by catechol, Soil Sci. Soc. Am. J. 65 (2001) 58–66.
[8] R.A. Petrie, P.R. Grossl, R.C. Sims, Oxidation of pentachlorophenol in manganese oxide suspensions under controlled *E*h and pH environments, Environ. Sci. Technol. 36 (2002) 3744–3748.
[9] H. Li, L.S. Lee, D.G. Schulze, C. Guest, Role of soil manganese in the oxidation of aromatic amines, Environ. Sci. Technol. 37 (2003) 2686–2693.
[10] H. Zhang, C.-H. Huang, Oxidative transformation of fluoroquinolone antibacterial agents and structurally related amines by manganese oxide, Environ. Sci. Technol. 39 (2005) 4474–4483.
[11] K.-H. Kang, D.-M. Lim, H. Shin, Oxidative-coupling reaction of TNT reduction products by manganese oxide, Water Res. 40 (2006) 903–910.
[12] H. Zhang, C.-H. Huang, Oxidative transformation of triclosan and chlorophene by manganese oxides, Environ. Sci. Technol. 37 (2003) 2421–2430.
[13] Y. Al-Degs, M.A. Khraisheh, M.F. Tutunji, Sorption of lead ions on diatomite and manganese oxides modified diatomite, Water Res. 35 (2001) 3724–3728.
[14] H.-J. Fan, P.R. Anderson, Copper and cadmium removal by Mn oxide-coated granular activated carbon, Sep. Purif. Technol. 45 (2005) 61–67.
[15] J. de Ruddera, T.V. de Wielea, W. Dhoogeb, F. Comhaireb, W. Verstraetea, Advanced water treatment with manganese oxide for the removal of 17α-ethynylestradiol (EE2), Water Res. 38 (2004) 184–192.
[16] G.M. Hettiarachchi, G.M. Pierzynski, M.D. Ransom, In situ stabilization of soil lead using phosphorus and manganese oxide, Environ. Sci. Technol. 34 (2000) 4614–4619.
[17] J. Ge, J. Qu, Degradation of azo dye acid red B on manganese dioxide in the absence and presence of ultrasonic irradiation, J. Hazard. Mater. B 100 (2003) 197–207.
[18] R. Liu, H. Tang, Oxidative decolorization of direct light red F3B dye at natural manganese mineral surface, Water Res. 34 (2000) 4029–4035.
[19] E. Deschamps, V.S.T. Ciminelli, W.H. Höll, Removal of As(III) and As(V) from water using a natural Fe and Mn enriched sample, Water Res. 39 (2005) 5212–5220.
[20] L.-J. Zhang, The black riddle on the sea floor: pelagite, Earth 15 (2004) 12–13 (in Chinese).
[21] J.E. Post, Manganese oxide minerals: crystal structures and economic and environmental significance, Proc. Natl. Acad. Sci. USA 96 (1999) 3447–3454.
[22] K. Parida, P.K. Satapathy, N. Das, Studies on Indian Ocean manganese nodules IV. Adsorption of some bivalent heavy metal ions onto ferromanganese nodules, J. Colloid Interface Sci. 181 (1996) 456–462.
[23] K.M. Parida, B. Gorac, N.N. Das, Studies on Indian Ocean manganese nodules III. Adsorption of aqueous selenite on ferromanganese nodules, J. Colloid Interface Sci. 187 (1997) 375–380.
[24] K.M. Parida, S. Mohanty, Studies on Indian Ocean manganese nodules VIII. Adsorption of aqueous phosphate on ferromanganese nodules, J. Colloid Interface Sci. 199 (1998) 22–27.
[25] S. Bhattacharjee, S. Chakrabarty, S. Maity, S. Kar, P. Thakur, G. Bhattacharyya, Removal of lead from contaminated water bodies using sea nodule as an adsorbent, Water Res. 37 (2004) 3954–3966.
[26] A. Agrawal, K.K. Sahu, B.D. Pandey, Systematic studies on adsorption of lead on sea nodule residues, J Colloid Interface Sci. 281 (2005) 291–298.
[27] J.-Q. Chen, D. Wang, M.-X. Zhu, C.-J. Gao, Study on degradation of methyl orange using pelagite as photocatalyst, J. Hazard. Mater. B 138 (2006) 182–186.
[28] S.-Q. Guo, W.-H. Sun, Mineralogy of Manganese Nodule of the Middle Pacific Ocean, Ocean Press, Beijing, 2006 (in Chinese).
[29] A.T. Stone, J.J. Morgan, Reduction and dissolution of manganese(III) and manganese(IV) oxides by organics. 1. Reaction with hydroquinone, Environ. Sci. Technol. 18 (1984) 450–456.
[30] J. Hong, C. Sun, S.-G. Yang, Y.-Z. Liu, Photocatalytic degradation of methylene blue in TiO_2 aqueous suspensions using microwave powered electrodeless discharge lamps, J. Hazard. Mater. B 133 (2006) 162–166.
[31] T.-C. An, X.-H. Zhu, Y. Xiong, Feasibility study of photoelectrochemical degradation of methylene blue with three-dimensional electrode-photocatalytic reactor, Chemosphere 46 (2002) 897–903.
[32] W. Stumm, J.J. Morgan, Aquatic Chemistry, third ed., Wiley, New York, 1996.
[33] D.M. Sherman, Electronic structures of iron(III) and manganese(IV) (hydro)oxide minerals: thermodynamics of photochemical reductive dissolution in aqueous environments, Geochim. Cosmochim. Acta 69 (2005) 3249–3255.

[34] Y. Wang, E.J. Reardon, Activation and regeneration of a soil sorbent for defluoridation of drinking water, Appl. Geochem. 16 (2001) 531–539.
[35] S. Laha, R.G. Luthy, Oxidation of aniline and other primary aromatic amines by manganese dioxide, Environ. Sci. Technol. 24 (1990) 363–373.
[36] Y.-S. Jun, C. Martin, Microscopic observations of reductive manganite dissolution under oxic conditions, Environ. Sci. Technol. 37 (2003) 2363–2370.
[37] A.T. Stone, Reduction dissolution of manganese(III/IV) oxides by substituted phenols, Environ. Sci. Technol. 21 (1987) 979–988.